

Assessment and Damping of Low Frequency Oscillations in Hybrid Power System due to Random Renewable Penetrations by Optimal FACTS Controllers

Narayan Nahak^{*‡}, Sankalpa Bohidar^{**}, Ranjan Kumar Mallick^{***}

^{*}Department of Electrical Engineering, ITER, Siksha ‘O’ Anusandhan Deemed to be University, India

^{**}Department of Electrical Engineering, ITER, Siksha ‘O’ Anusandhan Deemed to be University, India

^{***}Department of Electrical and Electronics Engineering, ITER, Siksha ‘O’ Anusandhan Deemed to be University, India

(narayannahak@soa.ac.in, sankalpabohidar@soa.ac.in, rkm.iter@gmail.com)

[‡]Corresponding Author; Narayan Nahak, Bhubaneswar, India, narayannahak@soa.ac.in

Received: 13.03.2020 Accepted:21.04.2020

Abstract- This paper presents a detail investigation on low frequency oscillations of a variable solar and wind penetrated power system. An optimized UPFC controller is proposed for damping low frequency oscillations to enhance small signal stability of such a power system. The modulation index of series converter and phase angle of shunt converters are controlled simultaneously in proposed UPFC controller there by incorporating the advantage of SSSC and STATCOM. The squirrel search algorithm (SSA) is proposed for tuning controller gains. The proposed UPFC controller has been compared with SSSC and STATCOM controllers to damp oscillations. Random variation of SPV, wind energy and their integration with varying synchronous generations has been considered in this work. It has been observed that increasing solar, variable wind and their interaction with variable synchronous power generation put more detrimental effect on low frequency power system oscillations. The detail time domain simulation and system eigen values predicted that proposed controller is able to damp these oscillations much efficiently for enhancing stability of such a critical power system.

Keywords Low frequency oscillations, solar photo voltaic, wind power source, UPFC, SSSC, STATCOM.

Nomenclature/Abbreviations

C_{dc}	Capacitance of dc link	X_d	d-axis steady state synchronous reactance for generator	V_b	Voltage of infinite bus
D	Coefficient of damping	X_E	Reactance for excitation transformer(ET)	V_{dc}	Voltage at the dc link
H	Inertia constant (MJ/MVA)	X_d'	d-axis transient synchronous reactance for generator	V_t	Generator terminal voltage
Ka, Ta	AVR gain and time constant	X_q	q-axis (quadrature axis) steady state synchronous reactance for generator	X_B	Reactance for the boosting transformer(BT)
$P_e = P_g$	Synchronous output power for generator	X_e	Total equivalent reactance for the system	X_{BV}	Reactance for the transmission line
P_i	Mechanical input power for generator	X_{TE}	Transformer reactance	T_{WG}, T_V	Time constants of wind and solar PV system
T_{d0}	Open circuit time constant of generator for d-axis(direct axis)	K_{WG}, K_V	Gains of wind and solar PV system	Φ_V	Solar irradiation(Kw/m ²)
V_w	Wind speed (m/s)	P_w	Wind turbine output power	P_{WG}	Wind energy generated power
FACTS	Flexible ac transmission system	SSSC	Static synchronous series compensator	STATCOM	Static synchronous compensator

UPFC	Unified power flow controller	SPV	Solar photo voltaic	SSA	Squirrel search algorithm
------	-------------------------------	-----	---------------------	-----	---------------------------

1. Introduction

Rotor angle stability is one of the important issues out of several issues of safe and reliable operation of power system. This aspect has been addressed in many researches in low and high frequency domain. The low frequency oscillation is becoming an all time issue, especially for a modern interconnected power system. The power system is on the path of integration with renewable sources to meet several challenges including depletion of fossil fuel. In [1, 2] power oscillation damping and impact on frequency dynamics being presented with low inertia system. Due to advancements in power generation, the cost of power generation from wind sources may be nearly same as from fossil fuel as per researches. Several researches have been conducted regarding integration of wind powers sources with conventional power generation [3]. In [4] Monte Carlo Simulation reveals bonding between power generation of wind and low frequency oscillatory stability and wind penetration on stability in [5]. In [6], it has been informed that the oscillatory stability would improve if conventional power source is replaced by wind sources but, specifically with constant power wind sources. But, the system oscillation would worsen with heavy wind power penetration as depicted in [7]. In [8] damping torque analysis has been performed to predict dynamic interaction of wind power source with synchronous generator. In SPV penetration has been continuously investigated by many researchers, which has been a challenging task for small signal stability [9, 10]. In [11] influence of grid impedance on low and high-Frequency Stability of PV generators being presented. The new MPPT schemes are presented in [12, 13] and novel solar cell power system being presented in [14]. As per [15], there should be a limit on SPV integration to power system for maintaining oscillatory stability. The increased SPV penetration adversely affects the critical mode of system oscillation. In [16] safety design feature has been presented with both wind and solar sources. In [17] the small signal stability studies have been performed by time domain simulation with different renewable sources. Hence as reported by different researchers, solar and wind penetration in large scale and in random manner detrimentally affects system oscillations. But, when both solar and wind penetrations have random variations, the system oscillations need more investigations, which has not been reported earlier, as per knowledge of author. In this article this issue has been investigated with a series of case studies.

Now the next issue is selection of a robust damping controller and an efficient control algorithm to tune the parameters of controller. The FACTS based controller has so many advantages over conventional PSS to damp oscillations. In [18], design and analysis of SSSC based Supplementary damping controller has been performed with real coded genetic algorithm and in [19] multi objective evolutionary technique being used for SSSC controller design. Coordinated multi input type SSSC controller with modified whale optimization algorithm technique is presented in [20].

Similarly coordinated damping control with STATCOM has been presented in [21]. In [22] imperial competitive algorithm is used for optimal STATCOM controller design. Also a detail analysis and assessment of STATCOM based stabilizer is being presented in [23] for stability enhancement of power system. But, as per literature [24, 25], UPFC is a multipurpose FACTS controller, which not only controls the power flow in transmission line but also efficiently damps power system oscillations. In [24] Heffron Phillips transfer function model of UPFC for assessing low frequency oscillations has been presented, but a systematic approach to design controller is explained in [25]. In [26] different robust control techniques were applied in decentralized UPFC controllers. In [27], firefly and cuckoo search algorithms being proposed based on UPFC for optimal location and dynamic stability enhancement of power system. As per [28] modulation indexes (m_B) along with phase angle (δ_E) are best UPFC control methods to damp oscillations. Hence in this work both m_B along with δ_E actions of UPFC are simultaneously controlled to enhance efficacy of UPFC. Next issue is selection of a suitable optimization technique to tune controller parameters. Different optimization techniques have been adopted by researchers to design UPFC based controller like modified salp swarm algorithm, PSO, IGWO, DE-PS, DE-PSO [29]-[32]. In [32], it has been stated that the design of UPFC based damping controller is an uphill task that needs more attention on a suitable control law or algorithm to tune controller gains. Recently a new nature inspired technique known as Squirrel search algorithm (SSA) has been proposed [33], which has been proven to provide accurate and consistent global optimum solution challenging to other prevailing techniques like PSO, FF, GA, MVO etc. Hence in this work SSA technique has been implemented and compared with other prevailing algorithms like DE, PSO, GWO and DEPSO. The prime contributions of this work can be summarized as:

- This work introduces a detail investigations on low frequency oscillations for step and random penetrations of wind and solar generations which are two important renewable sources and also their impact on synchronous generation output
- UPFC control action has been proposed to damp oscillations and compared with SSSC, STATCOM control actions
- SSA algorithm is proposed to tune controller gains, which has been compared with PSO, DE, DEPSO, GWO algorithms
- System response have been evaluated with detail time domain simulations and eigen values analysis to justify the damping action of proposed optimal UPFC control action

2. Power System with UPFC

The SMIB system along with solar and wind generations connected to UPFC is given in Fig.1, where IEEE-ST1A excitation system has been implemented. The UPFC variables are m_B , δ_B , m_E and δ_E . By controlling these variables the power system operation and control can be achieved.

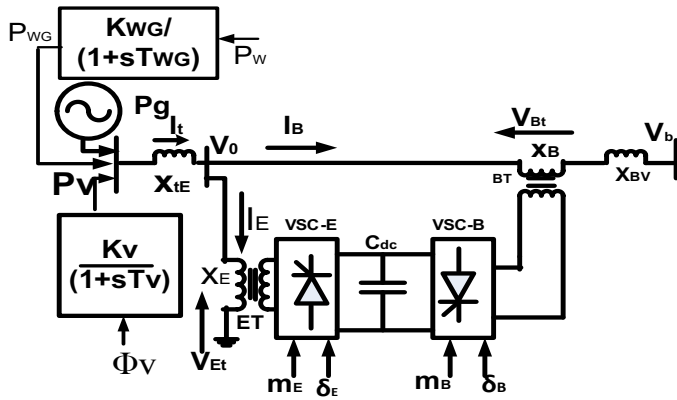


Fig.1. Power system integrated with solar and wind sources

3. Dynamic Model of the System Including UPFC

3.1. Non linear modeling of power system with only UPFC

The non linear modeling of only SMIB with UPFC is presented with following equations [25].

$$\dot{\omega} = \left(\frac{P_i - P_e - D\Delta\omega}{M} \right) \tag{1}$$

$$\delta = \omega_0(\omega - 1) \tag{2}$$

$$E'_q = (-E_q + E_{fd}) / T'_{d0} \tag{3}$$

$$E_{fd} = [-E_{fd} + K_a(V_{ref} - V_t)] / T_a \tag{4}$$

The dc link voltage is given by

$$\dot{V}_{dc} = \frac{3m_E}{4C_{dc}} (I_{Eq} \sin \delta_E + I_{Ed} \cos \delta_E) + \frac{3m_B}{4C_{dc}} (I_{Bq} \sin \delta_B + I_{Bd} \cos \delta_B) \tag{5}$$

Active power balance between the VSCs of UPFC is represented in Eq-(6) as

$$\text{Re}(V_B I_B^* - V_E I_E^*) = 0 \tag{6}$$

3.2. Linear modeling for dynamic study with UPFC

The linear modeling of power system around an operating point can be presented as: [25].

$$\dot{\Delta\delta} = \omega_0 \Delta\omega \tag{7}$$

And speed deviation is:

$$\Delta\omega = \left(\frac{-\Delta P_e - D\Delta\omega}{M} \right) \tag{8}$$

$$\Delta E'_q = (-\Delta E_q + \Delta E_{fd}) / T_{d0} \tag{9}$$

$$\Delta E_{fd} = [-\Delta E_{fd} + K_a(\Delta V_{ref} - \Delta V_t)] / T_a \tag{10}$$

$$\Delta V_{dc} = K_7 \Delta\delta + K_8 \Delta E'_q - K_q \Delta V_{dc} + K_{ce} \Delta m_E + K_{c\delta E} \Delta\delta_E + K_{cb} \Delta m_B + K_{c\delta B} \Delta\delta_B \tag{11}$$

Where, real power deviation is:

$$\Delta P_e = K_1 \Delta\delta + K_3 \Delta E'_q + K_{pd} \Delta V_{dc} + K_{pe} \Delta m_E + K_{p\delta E} \Delta\delta_E + K_{pb} \Delta m_B + K_{p\delta B} \Delta\delta_B \tag{12}$$

$$\Delta E_d = K_4 \Delta\delta + K_3 \Delta E'_q + K_{qd} \Delta V_{dc} + K_{qe} \Delta m_E + K_{q\delta E} \Delta\delta_E + K_{qb} \Delta m_B + K_{q\delta B} \Delta\delta_B \tag{13}$$

The terminal voltage is:

$$\Delta V_t = K_5 \Delta\delta + K_6 \Delta E'_q + K_{vd} \Delta V_{dc} + K_{ve} \Delta m_E + K_{v\delta E} \Delta\delta_E + K_{vb} \Delta m_B + K_{v\delta B} \Delta\delta_B \tag{14}$$

4. SPV Generation Modeling

The SPV generation, P_{spv} in watt can be presented as [17].

$$P_{spv} = \eta_c S_a \phi_v [1 - 0.005(T_a + 25)] \tag{15}$$

Here η_c and S_a being efficient and area are constant, so P_{spv} varies with T_a and ϕ_v , which are temperature and radiation. Temperature T_a is taken as 25°C. The modeling of SPV is represented by Fig.2.

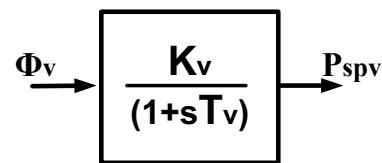


Fig.2. Modeling of SPV generation

5. Modeling of Wind Turbine Power

The wind speed V_w changes with coefficient C_p which is proportional to λ_p , tip speed ratio and β_p , the angle of blade pitch [17].

$$\lambda_p = \frac{R_b \omega_b}{V_w} \tag{16}$$

where, R_b is blade radius (23.5m.) and ω_b = blade speed (3.14rad/s). C_p is:

$$C_p = (0.44 - 0.0167\beta_p) \sin\left[\frac{\pi(\lambda_p - 3)}{15 - 0.3\beta_p}\right] - 0.0184(\lambda_p - 3)\beta_p \quad (17)$$

So the wind power is given by:

$$P_w = (1/2)\rho_a A_s C_p V_w^3 \quad (18)$$

Where ρ_a is air density ($=1.25 \text{ kg/m}^3$). A_s is blade swept area ($=1735\text{m}^2$) respectively. The wind generator modeling is given in Fig.3 and is depicted as in Eq-19.

$$G_{WG} = \frac{K_{WG}}{1 + sT_{WG}} = \frac{\Delta P_{WG}}{\Delta P_w} \quad (19)$$

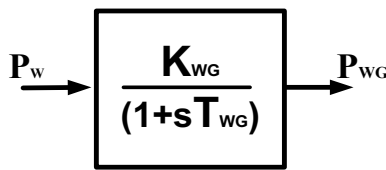


Fig.3. Modeling of wind generator system

6. Small Signal Model of Power System with UPFC

The small signal Heffron Phillips model as in Fig.4 consists of 28 constants being calculated at normal operating conditions [25]. The single machine system’s nominal data is being given in the appendix. Input $[\Delta U]$ being fed from external control action and $[K_{pu}]$, $[K_{vu}]$, $[K_{qu}]$ represent UPFC.

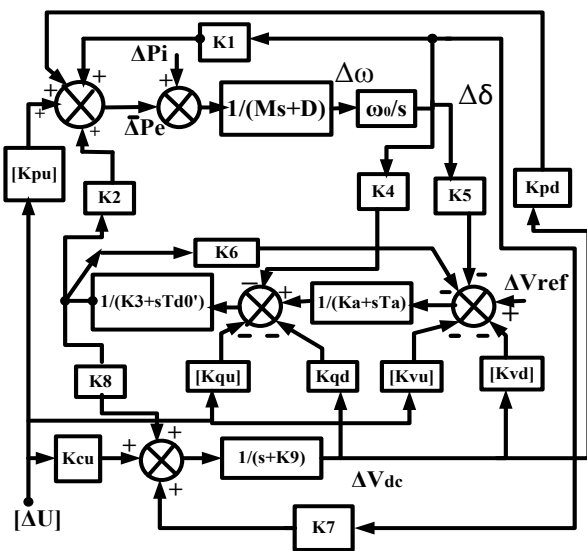


Fig.4. Modification of Heffron-Phillips model including UPFC

7. Controller Structure and Objective Function

The controller configuration is presented in Fig.5. For STATCOM and SSSC based controller, only the modulation index of voltage source converter (VSC) has been implemented. For UPFC, both series modulation index VSC (m_B) along with shunt phase angle VSC (δ_E) have been simultaneously implemented so as to consider the simultaneous action of both STATCOM and SSSC. Both the actions of UPFC are implemented in parallel to create damping

torque. Here K_{mb} , T_{mb1} , T_{mb2} being parameters to control modulation index of UPFC and K_{de} , T_{de1} , T_{de2} are parameters to control phase angle of UPFC controller. In this work ITAE objective function has been taken as given by Eq-(20) for which change in speed of generator being taken as input signal.

$$J = \int_0^{t_{sim}} t |\Delta \omega| dt \quad (20)$$

J is to be minimized considering the constraints in parameters. The gains range is taken from 1 to 100 for K_p , K_{mb} , K_{de} and time constants from 0.01 to 1 for $T_1, T_2, T_{mb1}, T_{mb2}, T_{de1}, T_{de2}$.

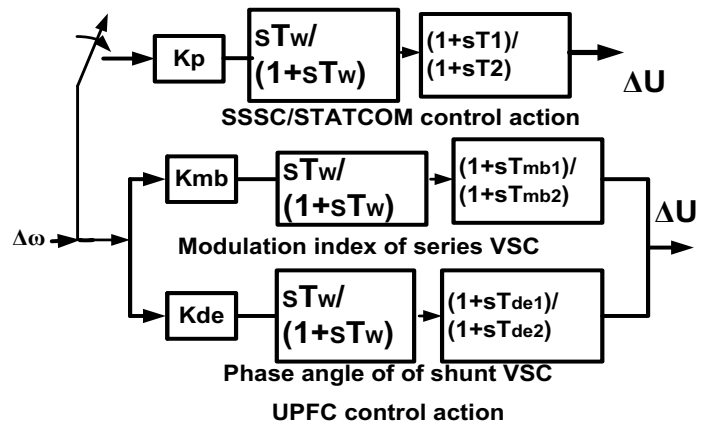


Fig.5. Controller structure

8. SSA Algorithm

It is a recently proposed optimization which is mostly inspired by nature [33]. The efficient moving way and the manners of southern flying squirrels is followed by this optimizer. The small mammals fly large distances very fast and are very efficient. They use a novel method of moving (i.e., Gliding). The squirrels search for food resources optimally when they start foraging dynamically. The SSA steps are as follows: (a) Number of squirrels flying in the forest are assumed to be n , (b) every squirrel flying utilize the available food resources in a dynamical manner by searching their food and (c) several varieties of trees (e.g., acorn, hickory and normal tree). The SSA pseudo code can be presented by following steps

Beginning:

- Defining input parameters.
- Number of flying squirrels n which represents the i^{th} squirrel and j^{th} dimension (i.e., numbering problem variables) in 't' iteration is generated randomly with the initial population. The parameters are again initialized.

$$FS_i = FS_L + U(0,1) \times (FS_u - FS_L) \quad (21)$$

- Flying squirrel position fitness being evaluated and sorted in ascend manner.
- Declaration of the flying squirrel.
- Selection of squirrel in random manner to be on normal tree moving to hickory tree and rest moving to acorn tree.

While (not satisfying the stopping criterion)

For $t = 1$ to $n1$ ($n1 = \text{No. of flying squirrels in all to be on acorn trees and moving to hickory tree}$)

if $r_1 \geq Pdp$

$$(FS^{t+1}_{i,j})_{at} = \left\{ (FS^t_{i,j})_{at} + d_g(G_c)((FS^t_{i,j})_{at} - (FS^t_{i,j})_{at}) \right\} \quad (22)$$

Where, d_g -gliding distance randomly, G_c -gliding constant based on exploration and exploitation of search space controlled, $r1$ uniform distribution of number randomly within range limit $[0, 1]$.

else

$(FS^{t+1}_{i,j})_{at}$ =location for random search space.

end

end

For $t = 1$ to $n2$ ($n2 = \text{sum of squirrels that are on normal trees and moving to acorn trees}$)

if $r_2 \geq Pdp$

$$(FS^{t+1}_{i,j})_{mt} = \left\{ (FS^t_{i,j})_{mt} + d_g(G_c)((FS^t_{i,j})_{mt} - (FS^t_{i,j})_{mt}) \right\} \quad (23)$$

Where $r2$ - uniform distribution of number randomly within range limit $[0, 1]$.

else

$(FS^{t+1}_{i,j})_{mt}$ = location for random search space.

end

end

if $r_3 \geq Pdp$

$$(FS^{t+1}_{i,j})_{mt} = \left\{ (FS^t_{i,j})_{mt} + d_g(G_c)((FS^t_{i,j})_{mt} - (FS^t_{i,j})_{mt}) \right\} \quad (24)$$

Where $r3$ is uniform distribution of number randomly within range limit $[0, 1]$.

else

$(FS^{t+1}_{i,j})_{mt}$ =location for random search space.

end

end

Calculating seasonal constant (S_c)

if (satisfying the seasonal monitoring condition)

Relocating randomly flying squirrels.

end

Updating the seasonal constant minimum value (S_{min})

end

The final optimal solution is the squirrel's location on hickory tree.

end

For checking terminating condition, flying squirrels' values and positions are calculated and updated at every iteration, till top position is reached. The squirrel's location on a hickory tree is reporting to be the final optimal solution which is represented as the best solution so far.

The flowchart of SSA algorithm is presented in Fig.6

9. Case Studies with Single Machine Integrated Power System

To investigate the impact of variable wind and solar penetration, a series of case studies have been conducted. These case studies include fix SPV with varying wind generation, fix wind with varying SPV and variable

synchronous generation in presence of wind and SPV sources. SSSC, STATCOM and UPFC simultaneous controller has been employed for enhancing dynamic stability of power system. The initial operating condition taken here is, $P_e = 0.8$ p.u. and $Q_e = 0.17$ p.u. The objective function for optimization is of ITAE type as given in Eq-20, for which a step change in 10% to input prime mover power has been taken.

9.1. Case-1-Constant Solar with Variable Wind Power Generation

Here, synchronous generation P_g is being fixed at 0.3 pu, solar generation P_v is kept fixed at 0.1 pu. The generation from wind source P_{wg} is step raised from 0 to 0.4 pu. The proposed UPFC controller and SSSC, STATCOM controller have been applied to create damping torque. A thorough comparison is done between proposed controllers, STATCOM along with SSSC based controller action as shown in Fig. 7, where the oscillation peaks and settling times are much reduced with SSA algorithm and UPFC control action proposed. The oscillation being aggravating without control action. The gains and time constants of the controllers are tuned by different control techniques like DE, PSO, DEPSO, GWO and compared with SSA. The optimal parameters and system eigen (SE) values are given in Table1 and Table 2 respectively. This table predicts that the mechanical modes have less imaginary part and more negative real part with proposed SSA-UPFC control action showing relatively improved stability. The critical oscillatory eigen value is $-0.9957 \pm 1.0905i$ for this condition with proposed controller. In this case all the algorithms along with SSA have been implemented with UPFC control actions and single lead-lag based STATCOM, SSSC control action for a broader comparison. The analysis of speed deviations and eigen values justify that UPFC being more versatile as compared to SSSC and STATCOM and also the investigation predicts the oscillations to be enhanced with sudden SPV penetration.

9.2. Case-2- Constant Wind with Variable Solar Power Generation

Here P_g , synchronous generation is being fixed at 0.3 pu as in earlier case, wind generation P_{wg} is kept fixed at 0.1 pu. The generation from solar source P_v is step raised from 0 to 0.4 pu. The proposed UPFC controller and SSSC, STATCOM controller have been applied to create damping torque. The performance of DEPSO technique has been found to be better than other (DE and PSO) techniques as found in previous case so in further studies, this technique has been considered. The system eigen values and system responses are shown in respective manner in Table 3 and Fig. 8. Dynamic stability of power system is affected by the change in real power output of SPV generation as predicted by results and oscillations being more aggravated in this condition. The critical oscillatory eigen value is $-3.3475 \pm 2.1462i$ for this condition with proposed action. The investigation on eigen values predict the oscillations to be enhanced with sudden wind penetration.

9.3. Case-3- Constant Wind and Solar Power with Variable Synchronous Power Generation

Here, synchronous power varies with wind and solar power generations. The P_g decreases from 0.8 pu, to 0.6 pu and 0.4pu and the values for $P_v = P_{wg} = 0.6$ pu. For deviations in speed and real power output of generator, system responses are given in a respective manner in Fig. 9 and Fig. 10. Table 4

and Table 5 show the SE values along with optimized parameters respectively. Taking into account hybrid (wind along with solar) power sources, having reduced synchronous power generation, the system oscillations are more excited which is predicted by the system response and eigen values. This is observed that the SE values of critical mode are $-3.3016 \pm 2.6548i$, $-1.9921 \pm 2.7220i$ and $-1.4586 \pm 4.1113i$ with $P_g=0.8, 0.6$ and $0.4pu$ respectively. In this case, to justify the better performance of UPFC controller, the SSA optimized

STATCOM and SSSC controller actions being compared with proposed controller. From different case studies it has been observed that critical system eigen values have comparatively less real part and more imaginary part with sudden variation of synchronous, solar and wind power generations by large amount thereby enhancing oscillatory response of system. This case also proved that with variations in generator output, low frequency oscillations are more enhanced in presence of renewable sources.

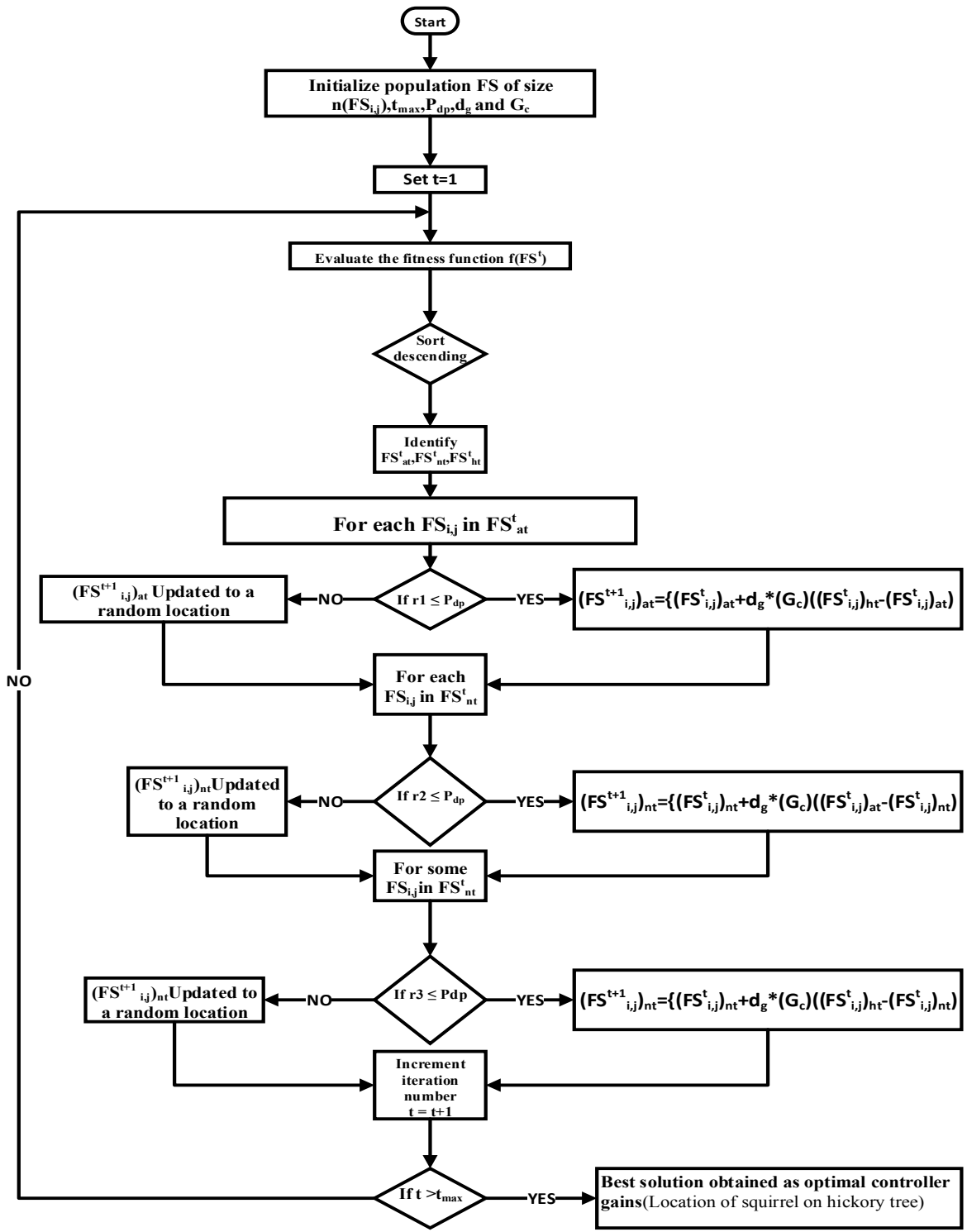


Fig.6. Flow chart of SSA Algorithm

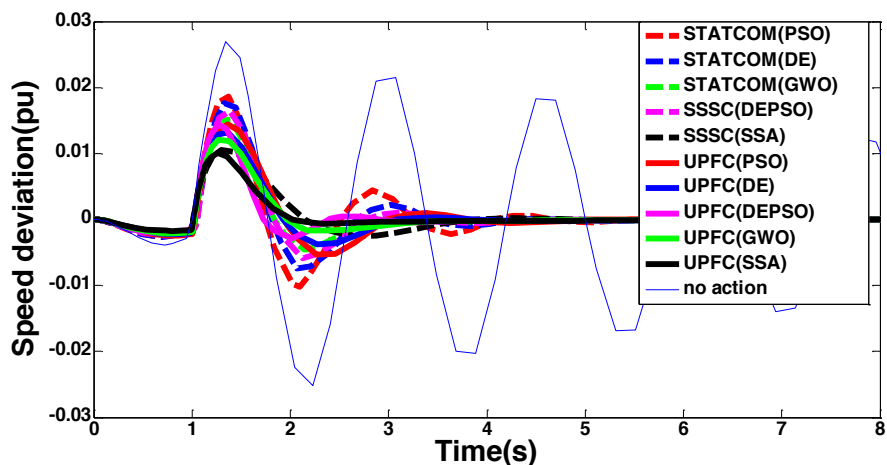


Fig.7. Sp. Deviation for cond-1 with constant SPV

Table 2. Optimized parameters

Control law Pw=0.4 pu	Single lead-lag controller K _p , T ₁ , T ₂	UPFC controller	
		K _{mb} , T _{mb1} , T _{mb2}	K _{de1} , T _{de1} , T _{de2}
SSA	33.9611, 0.8153, 0.3397 (SSSC)	50.5011, 0.2181, 0.1179	76.1813, 0.4064, 0.5543
DEPSO	39.7101, 0.6521, 0.8691 (SSSC)	33.7532, 0.1090, 0.6094	59.4899, 0.1035, 0.2464
GWO	38.4144, 0.1324, 0.1632 (STATCOM)	58.5402, 0.7439, 0.5279	33.1267, 0.5745, 0.4757
DE	36.5694, 0.4397, 0.6984 (STATCOM)	78.9365, 0.7126, 0.2707	28.0773, 0.3854, 0.8346
Control law Pw=0.6 pu	Single lead-lag controller K _p , T ₁ , T ₂	UPFC controller	
		K _{mb} , T _{mb1} , T _{mb2}	K _{de1} , T _{de1} , T _{de2}
SSA	38.5031, 0.5208, 0.4222 (SSSC)	31.2553, 0.9389, 0. 5278	74.9618, 0.6382, 0.5215
DEPSO	27.7861, 0.7795, 0.6356 (SSSC)	27.9159, 0.6881, 0.8044	29.693, 0.8525, 0.4092
GWO	80.137, 0.3612, 0.8371 (STATCOM)	90.0657, 0.4072, 0.5192	51.241, 0.4666, 0.4179
DE	60, 0.1793, 0.4962 (STATCOM)	31.1012, 0.9550, 0.8510	28.6571, 0.7082, 0.4896
PSO	20.2254, 0.7171, 0.1679 (STATCOM)	34.9930, 0.3257, 0.7089	16.9342, 0.9718, 0.3685

Table 3. Case-1, System eigen values

Operating Condition(pu)	PSO (STATCOM)	DE (STATCOM)	DE-PSO (SSSC)	GWO (STATCOM)	SSA (SSSC)
Pg=0.3 Pv=0.1 Pw=0.4	-99.834 -0.873 + 4.476i -0.874 - 4.476i -0.765 -0.511 -0.002 -0.103 0.0 -0.556 -0.667	-99.834 -1.138 + 4.129i -1.138 - 4.129i -1.260 -0.491 -0.002 -0.101 0.0 -0.556 -0.667	-99.833 -1.409 + 3.941i -1.409 - 3.941i -1.057 -0.492 -0.002 -0.102 0.0 -0.556 -0.667	-99.833 -5.367 -1.805 + 3.899i -1.805 - 3.899i -0.490 -0.002 -0.102 0.0 -0.556 -0.667	-99.832 -8.104 -1.158 + 2.144i -1.158 - 2.144i -0.487 -0.002 -0.102 0.0 -0.556 -0.667
Operating Condition(pu)	PSO UPFC	DE UPFC	DE-PSO UPFC	GWO UPFC	SSA UPFC
Pg=0.3 Pv=0.1 Pw=0.4	-99.835 -11.731 -1.151 + 3.304i -1.151 - 3.304i -2.488 -0.4866 -0.0018 -0.1017 -0.1000 0 -0.5556 -0.6667	-99.8346 -5.9299 -1.4657 + 3.0301i -1.4657 - 3.0301i -1.0629 -0.4892 -0.0018 -0.1025 -0.1000 0 -0.5556 -0.6667	-99.8334 -2.1404 + 2.3015i -2.1404 - 2.3015i -2.3541 -1.4519 -0.4966 -0.0018 -0.1036 -0.1000 0 -0.5556 -0.6667	-99.8334 -2.2667 + 2.6618i -2.2667 - 2.6618i -2.7012 -1.9535 -0.4875 -0.0018 -0.1024 -0.1000 0 -0.5556 -0.6667	-99.8331 -9.8388 -0.9957 + 1.0905i -0.9957 - 1.0905i -1.2862 -0.5037 -0.0018 -0.1048 -0.1000 0 -0.5556 -0.6667

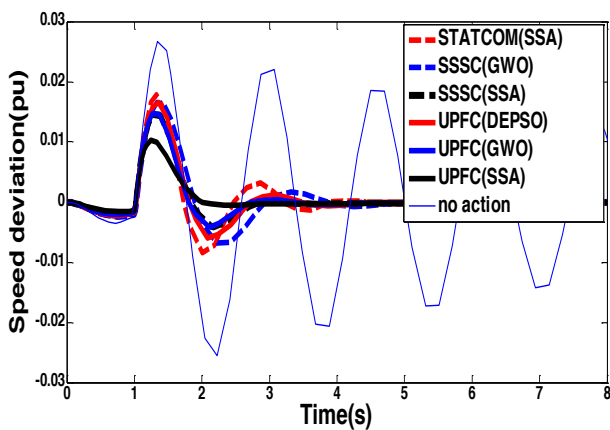


Fig.8. Sp. deviation for SMIB for cond-1 with constant wind generation

Table 4. Case-2, System eigen values

Operating Condition(pu)	SSA STATCOM	GWO SSSC	SSA SSSC
Pg=0.3 Pv=0.4 Pw=0.1	-99.834 -1.006 + 4.632i -1.006 - 4.632i -0.829 -0.513 -0.002 -0.104 0.0 -0.556 -0.667	-99.833 -1.158 + 3.317i -1.158 - 3.317i -3.396 -0.484 -0.002 -0.101 0.0 -0.556 -0.667	-99.833 -1.809 + 2.806i -1.809 - 2.806i -2.195 -0.491 -0.002 -0.102 0.0 -0.556 -0.667
Operating Condition(pu)	DE-PSO UPFC	GWO UPFC	SSA UPFC
Pg=0.3 Pv=0.4 Pw=0.1	-99.833 -1.369 + 3.973i	-99.833 -1.775 + 4.053i	-99.833 -3.3475 ± 2.1462i

-1.369-3.973i	-1.775 - 4.053i	-1.459 - 1.164
-3.749 - 1.106	-2.197 - 1.104	-0.504 - 0.002
-0.493 - 0.002	-0.493 - 0.002	-0.105 - 0.100
-0.102 - 0.100	-0.103 - 0.100	0.0 - 0.556
0.0 - 0.556	0.0 - 0.556	-0.667
-0.667	-0.667	

-0.7734 - 4.169i	4.099i	-1.224
-1.323 - 0.488	-0.648 - 4.099i	-1.001 - 0.492
-0.002 - 0.101	-2.136 - 0.485	-0.002 - 0.103
0.0 - 0.556	-0.002 - 0.101	-0.100 - 0.0
-0.667	0.0 - 0.556	0.0 - 0.556
	-0.667	-0.667

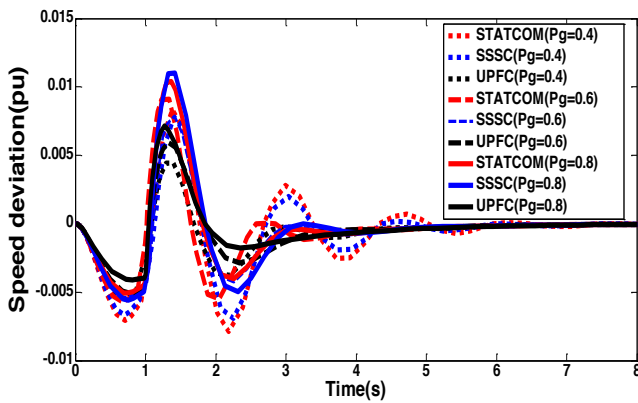


Fig.9. Speed deviation with varying Pg

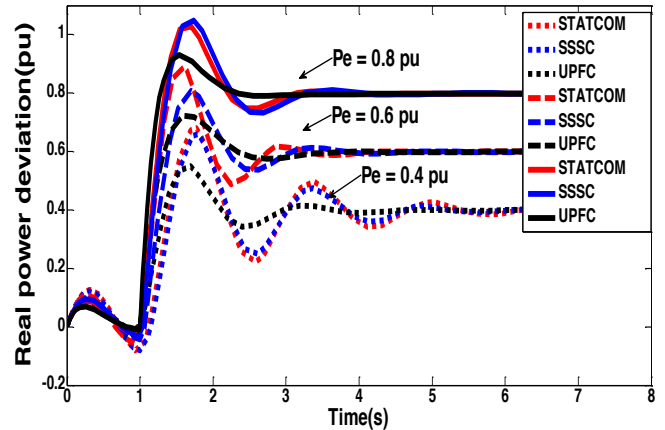


Fig.10 Real power deviation with varying Pg

Table 5. Case-3, System eigen values

SSSC	STATCOM	UPFC
Pg=0.8 pu		
-99.833	-99.833	-99.833
-1.657 + 3.455i	-1.957 + 3.654i	-3.3016 ± 2.6548i
-1.657 - 3.455i	-1.957 - 3.654i	-2.054
-2.052	-1.044	-1.829
-0.488	-0.495	-0.495
-0.002	-0.002	-0.002
-0.102	-0.103	-0.104
0.0	0.0	-0.100
-0.556	-0.556	0.0
-0.667	-0.667	-0.556
		-0.667
Pg=0.6 pu		
-99.8331	-99.834	-99.833
-1.647 + 3.873i	-1.542 + 4.714i	-1.9921 ± 2.7220i
-1.647 - 3.873i	-1.542 - 4.714i	-4.084
-1.343	-3.613	-2.186
-0.492	-0.490	-0.487
-0.002	-0.002	-0.002
-0.102	-0.102	-0.102
0.0	0.0	-0.100
-0.556	-0.556	0.0
-0.667	-0.667	-0.556
		-0.667
Pg=0.4 pu		
-99.834	-99.834	-99.833
-0.773 + 4.169i	-0.648 +	-1.4586 ± 4.1113i

Table 6. Case-3, Optimized parameters

Conditions	STATCOM controller	SSSC controller	UPFC controller	
	Kp, T1, T2	Kp, T1, T2	KB, TB1, TB2	KE, TE1, TE2
Pg=0.8 pu	39.292, 1, 1	50.022, 1, 1	77.561, 0.348, 0.461	58.721, 0.494, 1
Pg=0.6 pu	43.500, 1, 1	38.088, 1, 0.182	18.835, 0.448, 0.272	31.840, 1, 0.591
Pg=0.4 pu	26.097, 0.407, 1	16.726, 0.353, 0.449	51.536, 0.246, 1	40.896, 1, 1

10. Multi Machine Power System with Random Variations in P_{wg} along with P_v

Here, a multimachine hybrid (solar and wind) integrated PS as shown in Fig.11 has been considered. The UPFC VSCs are simultaneously applied with m_B and δ_E actions, whose parameters being tuned by SSA technique. Here two conditions have been investigated. In condition-1, the wind output power P_{wg} has been fixed at 0.2 p.u. and the solar output power P_{spv} being changed in random manner which is shown in Fig.12. Responses are presented in Fig.13 for ω₁₃ and in Fig.14 for ω₁₂. In condition-2, P_{spv} being varied

randomly as in Fig.12 with P_{wg} kept fixed at 0.2 p.u. and response given in Fig.15 for ω_{13} and in Fig.16 for ω_{12} . For both condition SSSC, UPFC controller have been applied. The response predicts that UPFC controller with m_B along with δ_E actions simultaneously damp oscillations much efficiently. A maximum delay of 50 ms is taken to access remote signal $\Delta\omega$ from each generator.

10.1. Condition-1

For condition-1, at $t=0s$, the output power of synchronous generator is increased by $P_g=0.8$ pu, the solar power, P_v is increased to 0.2 pu and the P_{wg} , wind power is varying in a randomly pattern as in Fig. 12. For investigation and damping resulting oscillations, time domain simulation is done for 100s. For damping oscillations DEPSO, GWO and proposed SSA optimized UPFC controllers have been employed and results being compared with SSA optimized SSSC controller.

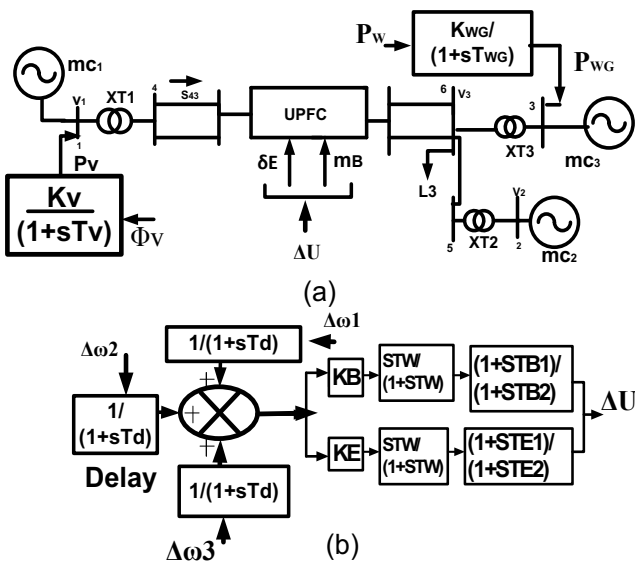


Fig.11. (a) Multi machine system, (b) Damping controller with multi inputs

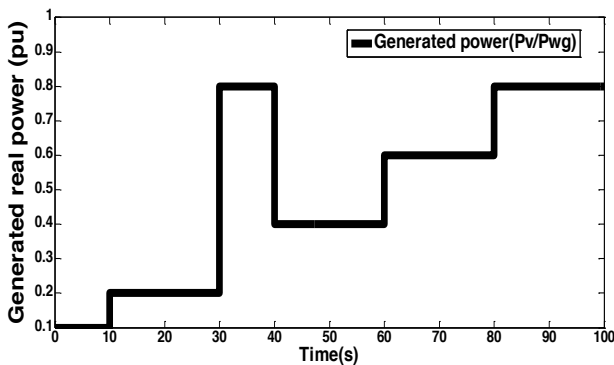


Fig.12. Case-4, conditions-1 and 2, random P_v and P_{wg} variations

10.2. Condition-2

For condition-2, at $t=0s$, output power of the synchronous generator is increased to $P_g=0.8$ pu and P_{wg} , the wind power, at $t=0s$, is increased to 0.2 pu and the P_v , solar

power is changing in the equal way as in condition-1 as in Fig. 12. To damp oscillations, the same controllers are used as in condition-1. It is seen that in case-4 in 0 -10s, due to continuous variations of synchronous and asynchronous generations, instigations of oscillations occur. By the use of proposed controller as compared to DEPSO, GWO along with SSA optimized UPFC and SSA optimized SSSC based controller, the system oscillations are damped adequately.

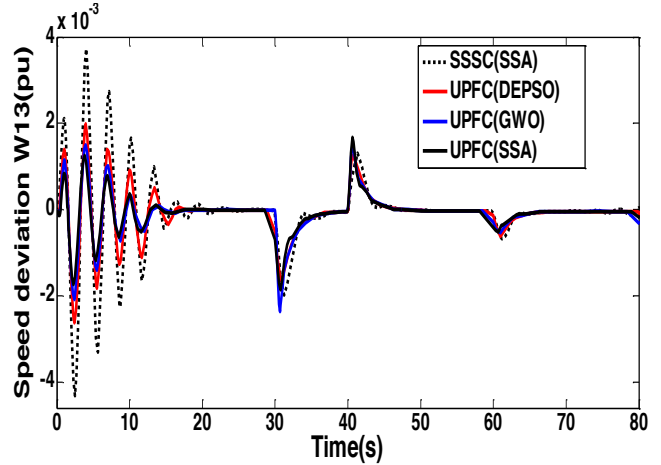


Fig.13. C-4, con.-1, Inter area oscillation ω_{13}

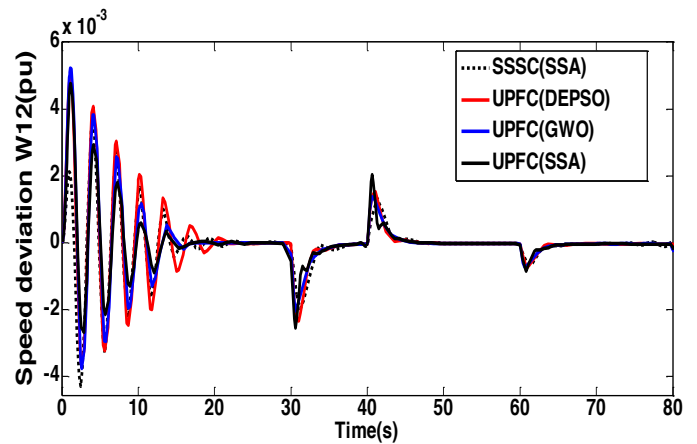


Fig.14. Cond.-1 Inter area oscillation ω_{12}

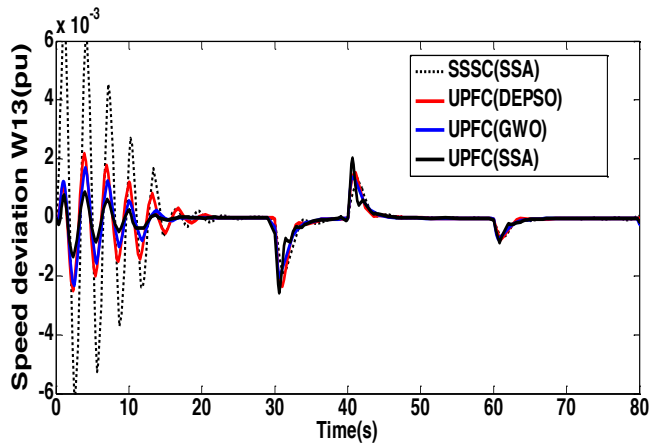


Fig.15. Cond.-2, Inter area oscillation ω_{13}

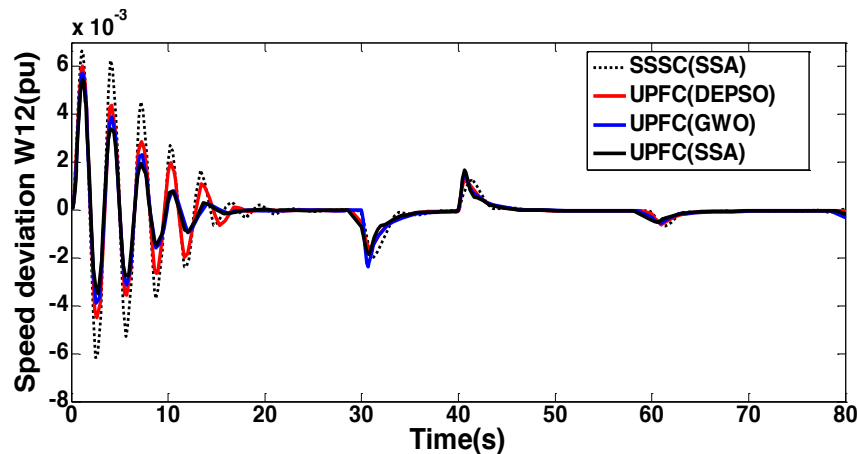


Fig.16. Cond.-2, Inter area oscillation ω_{12}

11. Conclusion

This work presented a comparative approach of proposed SSA optimized UPFC with optimal SSSC and STATCOM controller actions to enhance dynamic stability for a stochastic hybrid renewable (solar and wind) penetrated power system. This work has satisfied two objectives, first is investigations on low frequency oscillations by arbitrary wind and solar penetration and second is proposal of SSA tuned UPFC as damping controller. This work can be further extended to other renewable sources. Following conclusions obtained from this work.

- Random solar and wind penetrations put more detrimental effect on power system oscillations as compared to constant power source. Also for fixed solar and wind power generation, reduced synchronous generation instigates low frequency oscillations.
- System response and detail eigen value analysis with time domain simulations predict that proposed optimal UPFC controller is more versatile and damps system oscillations in a efficient manner in comparison to optimal SSSC along with STATCOM damping controller actions.
- The three machine system has been considered here only to justify the objective of this work. Maximum sensor and communication delay considered here shows that proposed controller can be employed to enhance dynamic stability of a large inter connected renewable integrated power system.

References

[1] M. Zarifakis, W. T. Coffey, Y. P. Kalmykov, S. V. Titov, D. J. Byrne and S. J. Carrig, "Active Damping of Power Oscillations Following Frequency Changes in Low Inertia Power Systems," in IEEE Transactions on Power Systems, vol. 34, no. 6, pp. 4984-4992, Nov. 2019.

[2] S. Favuzza, M. S. Navarro Navia, R. Musca, E. Riva Sanseverino, G. Zizzo, B. Doan Van and N. Nguyen

Quang, "Impact of RES Penetration on the Frequency Dynamics of the 500 kV Vietnamese Power System," 8th International Conference on Renewable Energy Research and Applications (ICRERA), Brasov, Romania, 2019, pp. 668-672.

[3] H. Yin, M. Dereschkewitz, D. Wagenitz and S. Dieckerhoff, "A versatile test bench for grid integration investigations of back-to-back wind energy conversion systems," International Conference on Renewable Energy Research and Application (ICRERA), Milwaukee, WI, 2014, pp. 695-700.

[4] L.B.Shi, C Wang, L.Z.Yao, L.M.Wang and Y.X.Ni "Analysis of impact of grid-connected wind power on small signal stability". *Wind Energy*. **2011**, *14*, 518–537.

[5] H. U. Banna, A. Luna, S. Ying, H. Ghorbani and P. Rodriguez, "Impacts of wind energy in-feed on power system small signal stability," *2014 International Conference on Renewable Energy Research and Application (ICRERA)*, Milwaukee, WI, 2014, pp. 615-622.

[6] J.G.Slootweg and W.L. Kling, "The impact of large scale wind power generation on power system oscillations". *Electr. Power Syst. Res.* **2003**, *67*, 9–20.

[7] Wenyong Liu, Rundong Ge, Huiyong Li and Jiangbei Ge, "Impact of Large-Scale Wind Power Integration on Small Signal Stability Based on Stability Region Boundary". *Sustainability* 2014, *6*, 7921-7944

[8] Ravi Bhushan and Kalyan Chatterjee. "Effects of parameter variation in DFIG-based grid connected system with a FACTS device for small-signal stability analysis". *IET Gener. Transm. Distrib.*, Vol. 11 Iss. 11, pp. 2762-2777, 2017

[9] Utpal Kumar Das, Kok Soon Tey, Mehdi Seyedmahmoudian, SaadMekhilef, Moh Yamani Idnaldris, Willem Van Deventer, Bend Horan and Alex Stojcevski, "Forecasting of photovoltaic power generation and model optimization: A review", *Renewable and Sustainable Energy Reviews* 81 (2018) 912–928.

[10] Y. T. Tan, D. S. Kirschen and N. Jenkins, "A model of PV generation suitable for stability analysis", *IEEE Trans. on Energy Conversion*, Vol.19, No.4, 2004, pp748-755

[11] Y. Xia, Y. Peng, P. Yang, Y. Li and W. Wei, "Different Influence of Grid Impedance on Low- and High-

- Frequency Stability of PV Generators," in IEEE Transactions on Industrial Electronics, vol. 66, no. 11, pp. 8498-8508, Nov. 2019.
- [12] K. Kajiwara, N. Matsui and F. Kurokawa, "A new MPPT control for solar panel under bus voltage fluctuation," 2017 IEEE 6th International Conference on Renewable Energy Research and Applications (ICRERA), San Diego, CA, 2017, pp. 1047-1050
- [13] N. Güler and E. Irmak, "MPPT Based Model Predictive Control of Grid Connected Inverter for PV Systems," 2019 8th International Conference on Renewable Energy Research and Applications (ICRERA), Brasov, Romania, 2019, pp. 982-986.
- [14] H. Matsuo and F. Kurokawa, "Novel solar cell power supply system using bidirectional dc-dc converter," Proc. IEEE Power Electron. Spec. Conf.(PESC), Cambridge, MA, Jun. 1982, pp. 14-19.
- [15] W. Du, H. F. Wang and R. Dunn, "Power System Small-Signal Oscillation Stability as Affected by Large-scale PV Penetration" International conference on Sustainable Power Generation and Supply, SUPERGEN-2009, China.
- [16] Veronica Melissa Salas-Mora and Gustavo Richmond-Navarro, "Safety Design of a Hybrid Wind-Solar Energy System for Rural Remote Areas in Costa Rica" International journal of renewable energy research, Vol.10, No.1, March, 2020.
- [17] Dong-Jing Lee and Li Wang, "Small-Signal Stability Analysis of an Autonomous Hybrid Renewable Energy Power Generation/Energy Storage System Part I: Time-Domain Simulations". IEEE Transactions on energy conversion, Vol. 23, No. 1, March 2008
- [18] S.Panda, S.C.Swain, P.K.Rautray, R.K.Malik and G.Panda, "Design and analysis of SSSC-based supplementary damping controller", Simulation Modelling Practice and Theory, Volume 18, Issue 9, October 2010, Pages 1199-1213
- [19] S Panda, "Multi-objective evolutionary algorithm for SSSC-based controller design, Electric Power Systems Research" 79 (6), 2009, 937-944
- [20] P.R. Sahu, P.K. Hota and S. Panda, "Modified whale optimization algorithm for fractional-order multi-input SSSC-based controller design". Optim Control Appl Meth. 2018; 39: 1802- 1817
- [21] Chunyi Guo, Wen Jiang and Chengyong Zhao, "Small-signal instability and supplementary coordinated damping-control of LCC-HVDC system with STATCOM under weak AC grid conditions", International Journal of Electrical Power & Energy Systems, Volume 104, January 2019, Pages 246-254
- [22] S. M. Abd-Elazim and E. S. Ali, "Imperialist competitive algorithm for optimal STATCOM design in a multimachine power system", International Journal of Electrical Power & Energy Systems, Volume 76, March 2016, Pages 136-146
- [23] M.A.Abido, "Analysis and assessment of STATCOM-based damping stabilizers for power system stability enhancement", Electric Power Systems Research, Volume 73, Issue 2, February 2005, Pages 177-185
- [24] H.F.Wang, "A unified model for the analysis of FACTS devices in damping power system oscillations – part III: unified power flow controller". IEEE Trans Power Deliver 2000;15(3):978-83.
- [25] N.Tambey and M.L. Kothari, "Damping of power system oscillations with unified power flow controller (UPFC)". IEE Proc Gener Trans Distrib 2003;150:129-40.
- [26] S.A. Taher, R.Hemmati, A. Abdolalipour and S. Akbari, "Comparison of different robust control methods in the design of decentralized UPFC controllers". Int J Electr Power Energy Syst 2012;43:173-84.
- [27] B.V. Kumar and N.V. Srikanth, "A hybrid approach for optimal location and capacity of UPFC to improve the dynamic stability of the power system", Appl. Soft Comput. J. (2016), <http://dx.doi.org/10.1016/j.asoc.2016.09.031>
- [28] R.K.Pandey and N.K.Singh, "UPFC control parameter identification for effective power oscillation damping", Electrical Power and Energy Systems 31 (2009) 269-276
- [29] B. Vijay Kumar and V. Ramaiah, "Enhancement of dynamic stability by optimal location and capacity of UPFC: A hybrid approach", Energy, Volume 190, 2020
- [30] Rabindra Kumar Sahu, Tulasi Chandra, Sekhar Gorripotu and Sidhartha Panda, "A hybrid DE-PS algorithm for load frequency control under deregulated power system with UPFC and RFB", Ain Shams Engineering Journal, Volume 6, Issue 3, 2015, 893-911,
- [31] R.K. Mallick and N. Nahak, "Hybrid differential evolution particle swarm optimization (DE-PSO) algorithm for optimization of unified power flow controller parameters", IEEE, UPCON-IIT BHU-2016, art. no. 7894729, pp. 635-640.
- [32] N. Nahak and R.K.Mallick, "Investigation and damping of low frequency oscillations of stochastic solar penetrated power system by optimal dual UPFC", IET Renewable Power Generation, 2019, Vol. 13 Iss. 3, pp. 376-388
- [33] Mohit Jain, Vijander Singh and Asha Rani, "A novel nature-inspired algorithm for optimization: Squirrel search algorithm", Swarm and Evolutionary Computation 44 (2019) 148-175

Appendix (All the data are in per unit except constants)

A. Single machine infinite bus test system data

$C_{dc}=1$, $H=4\text{MJ/MVA}$, $K_a=100$, $T_a=0.01$, $T_{d0}=5.044\text{sec}$, $D=0$, $\delta_0=47.13^\circ$, $V_b=1$, $V_{dc}=2$, $V_t=1$, $X_B=X_E=0.1$, $X_{BV}=0.3$, $X_d=1$, $X_d'=0.3$, $X_q=0.6$, $X_e=0.5$

B. Multimachine system data

$H_2=20$, $H_3=11.8$, $D_2=D_3=0$, $T'_{d02}=7.5\text{ sec}$, $T'_{d03}=4.7\text{ sec}$, $T_{dc}=0.01$, $K_{dc}=5$, $X_{q2}=0.16$, $X_{q3}=0.33$, $X_{d2}=0.19$, $X_{d3}=0.41$, $X'_{d2}=0.076$, $T_{A2}=0.01$, $K_{A2}=100$, $K_{A3}=20$, $T_{A2}=0.01$, $Z_{13}=j0.6(\text{double lines})$, $Z_{23}=j0.1$, $L_3=0.8-j1.253$, $V_3=1<0^\circ$, $V_2=1<5^\circ$

C. UPFC parameters :

$m_B=0.0789$, $m_E=0.4013$, $\delta_B=-78.2174^\circ$, $\delta_E=-85.3478^\circ$

D. Parameters of dc link : $V_{dc}=2\text{ pu}$, $C_{dc}=1\text{ pu}$

E. Parameters of solar and wind power sources

$K_V=1.0$, $T_V=1.8\text{ s}$, $K_{WG}=1.0$, $T_{WG}=1.5\text{ s}$